Pharmacology Biochemistry & Behavior, Vol. 40, pp. 503-507. © Pergamon Press plc, 1991. Printed in the U.S.A. 0091-3057/91 $3.00 + .00

PET Studies in the Primate Brain and Biodistribution in Mice Using (−)-5′-^{18}F-Δ^8-THC

A. CHARALAMBOUS,* G. MARCINIAK,* C.-Y. SHIUE,†‡ S. L. DEWEY,†
D. J. SCHLYER,† A. P. WOLF† AND A. MAKRIYANNIS*[1]

**Department of Medicinal Chemistry, School of Pharmacy, University of Connecticut, Storrs, CT 06269-2092*
†Brookhaven National Laboratory, Department of Chemistry, Upton, NY 11973
‡Creighton University, Center for Metabolic Imaging, Omaha, NE 68108

CHARALAMBOUS, A., G. MARCINIAK, C.-Y. SHIUE, S. L. DEWEY, D. J. SCHLYER, A. P. WOLF AND A. MAKRIYANNIS. *PET studies in the primate brain and biodistribution in mice using (−)-5′-^{18}F-Δ^8-THC.* PHARMACOL BIOCHEM BEHAV **40**(3) 503–507, 1991.—Cannabinoids, the active constituents of marijuana, are known to have many therapeutic properties; however, their exact mechanism of action is not well understood. In an effort to obtain more information concerning the pharmacokinetics and biodistribution of psychoactive THC analogs we synthesized (−)-^{18}F-Δ^8-THC and studied its biodistribution in mice and baboon brains. The analog was obtained by nucleophilic fluorination of the ditriflate ester of (−)-5′-OH-Δ^8-THC with K^{18}F/Kryptofix followed by deprotection with $LiAlH_4$ and purification with HPLC in 8% yield in a 90-min synthesis from EOB. The uptake of (−)-5′-^{18}F-Δ^8-THC in mouse tissue was high at 5 min, but radioactivity declined rapidly in almost all the tissues studied. Following IV administration, (−)-5′-^{18}F-Δ^8-THC uptake in baboon brain was similar in the basal ganglia, thalamus and cerebellum, and the clearance from these regions was relatively rapid. Also, a study from baboon plasma clearance of (−)-5′-^{18}F-Δ^8-THC showed rapid metabolism of the analog.

(−)-5′-^{18}F-Δ^8-THC Biodistribution PET

SINCE ancient times *Cannabis sativa* L. has been known for its many therapeutic properties and has been widely used in various preparations in folklore medicine (16). The active constituents of the plant, the cannabinoids, have numerous pharmacological properties including psychotropic effects, bronchodilation, increased heart rate, reduced intraocular pressure, analgesia, alteration of body temperature, anticonvulsant activity and others. (5).

Because of their high lipophilicity, cannabinoids are expected to partition preferentially in the hydrophobic component of the membrane thus affecting membrane-related functions either through lipid perturbation or through direct interaction with membrane-associated proteins, at catalytic or noncatalytic sites. Indeed, cannabinoids have been shown to affect a variety of membrane preparations including membrane-associated enzymes (13), brain synaptosomes (9), blood platelets (17), human lung fibroblasts (2), and numerous membrane-associated receptors (13). To understand the effects of cannabinoids on the membrane we have studied the topography, stereochemistry and dynamic features of these drug molecules in the membrane using deuterium solid-state NMR (11) and small angle x-ray diffraction (15).

Recently, it has been shown that at least some of the cannabinoid effects are due to interactions with specific binding sites. Evidence for such sites was obtained using the radioactive [^{3}H] CP-55,940 ligand, in cultured neuroblastoma cells (10) and in rat brain synaptosomal membranes (4) in both of which cannabinoids inhibit adenylate cyclase. Also, these sites have been visualized autoradiographically in the brain of several mammals including man (8). Recently, a complementary DNA isolated from the rat cortex has been cloned and expressed (14). This cDNA encodes for a cannabinoid receptor whose mRNA is found in cells and regions of the brain where the cannabinoid binding sites have been visualized.

In attempting to provide more information concerning the pharmacokinetics and biodistribution of psychoactive THC analogs, we synthesized ^{18}F-labeled (−)-5′-fluoro-Δ^8-THC and studied its biodistribution in mice. Also, we obtained information on its biodistribution in primate brain using positron emission tomography (PET). A preliminary report on these studies has already appeared (12).

We chose to work with (−)-5′-^{18}F-Δ^8-THC for the following reasons: a) The parent compound (−)-Δ^8-THC is among the most psychoactive and stable constituents of marijuana, b) the 5′ position has been reported to be less prone to metabolic

[1]Requests for reprints should be addressed to Alexandros Makriyannis, School of Pharmacy, U-92 University of Connecticut, Storrs, CT 06269-2092.

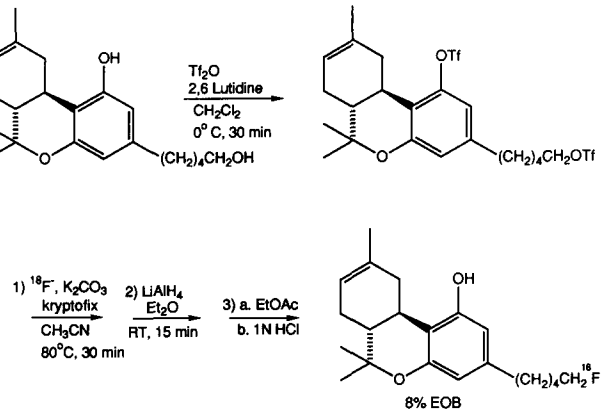

Scheme 1. Synthesis of (-)-5'-[^{18}F]-Δ^8-THC

modifications (1) and c) ^{18}F has a relatively long half-life when compared to the available positron emitting radioisotopes. Finally, when biological testing of the "cold" (−)-5′-fluoro-Δ^8-THC derivative found it to be almost equipotent to the parent compound (3), we felt confident in proceeding with the PET experiments.

PET is a technique which can be very effective for studying in vivo biochemical processes and the functional state of many organs. The technique involves labelling the molecule of biological interest with a short-lived positron-emitting radioisotope. After intravenous injection or inhalation, the distribution and concentration of the labeled molecule in regional tissues can be monitored (7). More specifically, the radioisotopes are produced in the cyclotron as small precursor molecules, $K^{18}F$ in our case, which because of their very short half-life (109.8 min for ^{18}F) must be rapidly incorporated into the molecule of biological interest. Since the specific activity of the radioisotope is very high (1.71×10^6 Ci/mmol for ^{18}F), small concentrations of compound are needed and, therefore, the compounds are synthesized in micromolar quantities. Finally, image reconstruction of the source that generates the radioactivity demonstrates the regional distribution and concentration of the radioactive molecule.

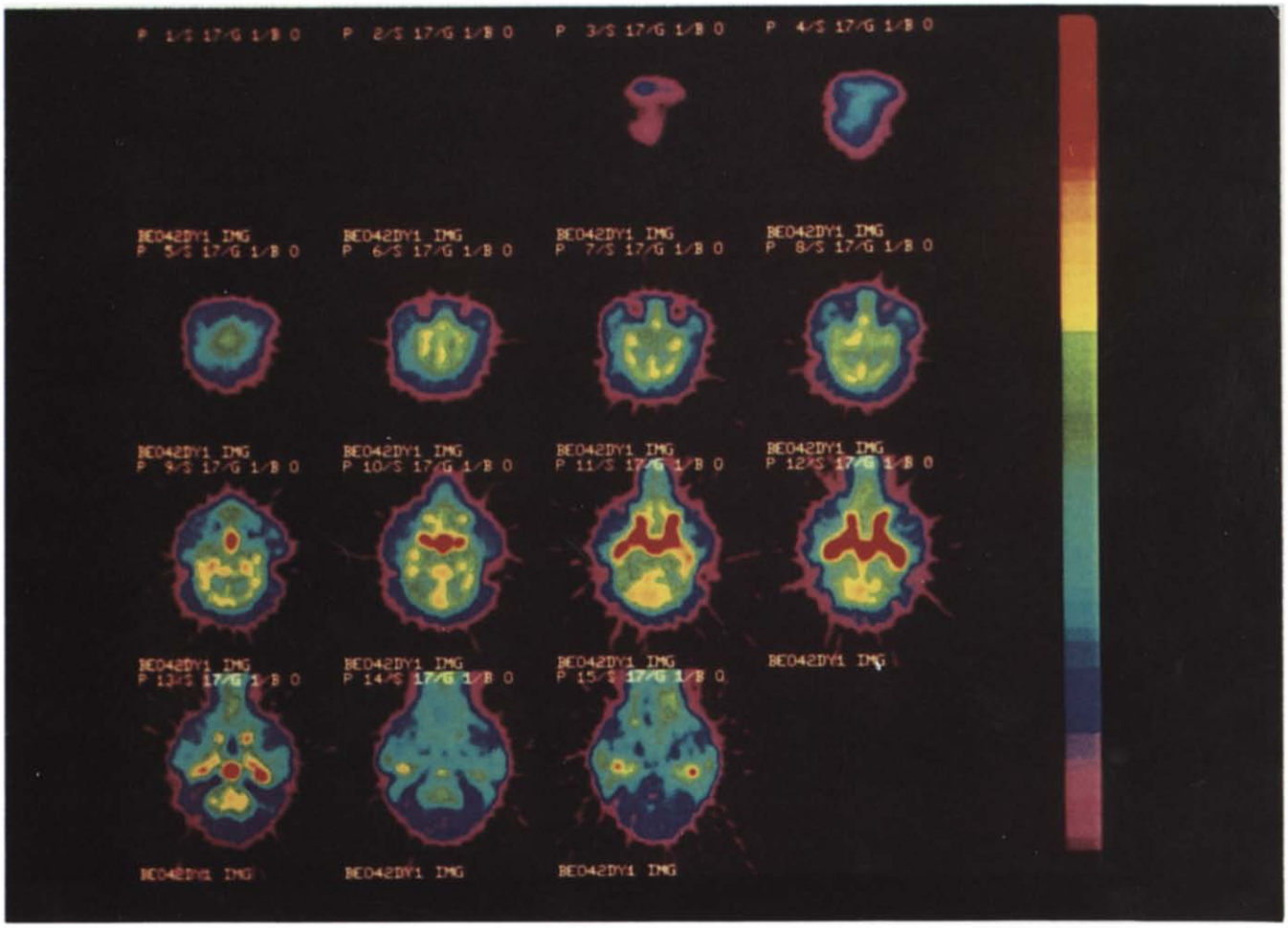

FIG. 1. Transaxial PET images taken 60 min after IV injection of (−)-5′-^{18}F-Δ^8-THC and through the rostral (top left) caudal (bottom right) extent of the baboon brain as described in the text.

TABLE 1

TISSUE DISTRIBUTION OF (−)-5′-^{18}F-Δ^{8}-THC IN MICE

	Mean ± S.E.M.(n = 4) Time After Injection					
	5 Minutes		30 Minutes		60 Minutes	
Organ	&/Organ	%/Gram	&/Organ	%/Gram	&/Organ	%/Gram
Brain	1.07 ± 0.14	2.23 ± 0.34	0.52 ± 0.05	1.07 ± 0.09	0.24 ± 0.01	0.52 ± 0.02
Blood	—	2.65 ± 0.21	—	2.27 ± 0.69	—	1.38 ± 0.12
Heart	0.88 ± 0.17	6.45 ± 1.10	0.19 ± 0.03	1.53 ± 0.15	0.10 ± 0.01	0.88 ± 0.06
Lungs	0.81 ± 0.12	4.82 ± 0.74	0.39 ± 0.17	1.72 ± 0.23	0.19 ± 0.05	1.15 ± 0.15
Liver	25.31 ± 2.73	20.07 ± 2.06	13.49 ± 7.90	9.08 ± 5.20	9.72 ± 0.60	7.44 ± 0.33
Spleen	0.41 ± 0.07	2.85 ± 0.43	0.16 ± 0.04	1.07 ± 0.09	0.10 ± 0.01	0.67 ± 0.09
Kidneys	3.17 ± 0.46	7.33 ± 0.85	0.75 ± 0.16	1.86 ± 0.26	0.41 ± 0.02	1.04 ± 0.08
Small Intes.	6.84 ± 2.74	3.42 ± 1.04	30.89 ± 13.6	16.08 ± 5.02	42.66 ± 20.2	22.92 ± 10.1
Femur	—	1.38 ± 0.31	—	1.50 ± 0.19	—	1.65 ± 0.26
Muscle	—	2.57 ± 0.30	—	1.06 ± 0.23	—	0.68 ± 0.19

CHEMISTRY

The synthetic route that we followed for obtaining (−)-5′-^{18}F-Δ^{8}-THC is shown in Scheme 1. (−)-5′-Hydroxyl-Δ^{8}-THC was synthesized according to a literature procedure (18) and was converted to the triflate diester through reaction with triflic anhydride in the presence of 2,6-lutidine, in methylene chloride at 0°C. Reaction of the ditriflate with K^{18}F and kryptofix in acetonitrile at 80°C provided the (−)-5′-^{18}F-Δ^{8}-THC triflic ester, which was converted to the free phenol without further purification using 1 M $LiAlH_4$ in ether solution. After acidification with 1 N HCl and ether extraction, the final product was purified using HPLC (Beckman Ultrasphere semipreparative silica gel column) and 5% ethyl acetate in hexanes as eluent; the yield was 8% for a 90-min synthesis from the end of bombardment (EOB). Finally, the solvent was evaporated and the compound was dissolved in a 5:5:90 ethanol:emulphor:saline solution for a final volume of 2.5 ml which after filtration through millipore was injected in the animals.

METHOD

Adult female mice (BNL strain, 26–31 g) received tail vein injections of ^{18}F-THC (24–72 μCi). At the appropriate times, animals were sacrificed by cervical dislocation. Tissues were rapidly removed, blotted free of excess blood, and counted for total radioactivity.

Adult female baboons (*Papio anubis*, 13.5–15.0 kg) were used for all PET studies and were prepared as described previously (6). Scanning was performed in a Computer Technology Imaging (CTI) positron tomograph (model 931-08/12; 15 slice, 6.5 m slice thickness, full width at half maximum (FWHM).

Baboon Plasma Metabolite Analysis

After each injection of radioligand blood was sampled from the femoral artery at 2.5-s intervals for the initial 2 min, via an automatic blood sampling device. Subsequent samples were drawn at discrete preselected time intervals up to the end of the study.

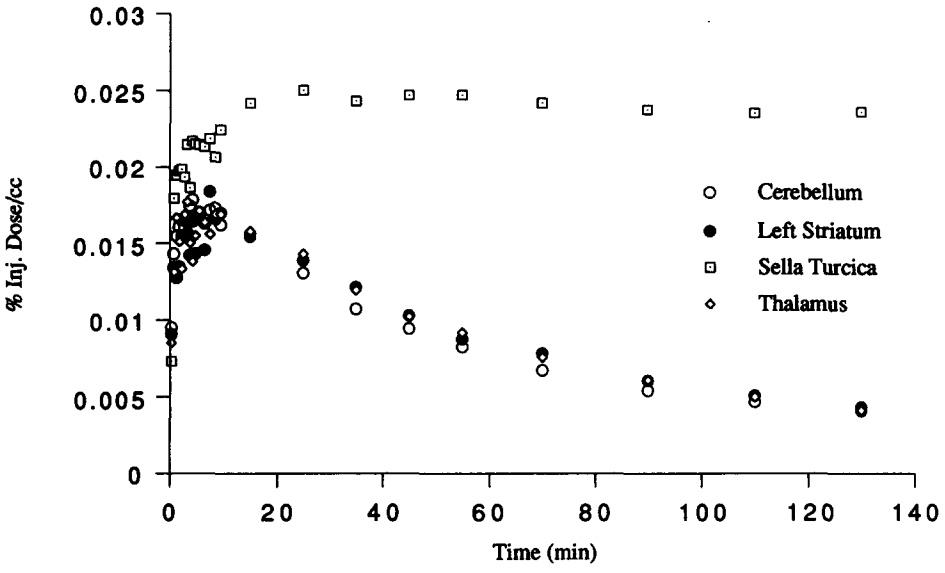

FIG. 2. Time courses for (−)-5′-^{18}F-Δ^{18}-THC distribution in baboon brain.

TABLE 2

ANALYSIS OF ^{18}F RADIOACTIVITY IN BABOON PLASMA SAMPLE*

Min. After Injection	% of ^{18}F Extracted From Plasma	% of ^{18}F in MeOH as ^{18}F-THC	% of Unchanged ^{18}F-THC
0.67	95	97.7	92.8
	(92.7; 97.2)	(97.3; 98.1)	(90.2; 95.4)
4	86.7	67.2	58.3
	(86.6; 86.8)	(62.0;72.3)	(53.7; 62.8)
10	83.6	32.3	27.0
	(83.3; 83.8)	(27.7; 36.8)	(23.1; 30.8)
30	82.4	17.9	15.0
	(81.1; 83.7)	(16.6;19.2)	(13.5;16.1)
60	79.6	15.8	13.0
	(77.2; 82.0)	(12.8: 18.8)	(10.0; 15.4)
120	76.9	15.3	12.0
	(75.3; 78.4)	(11.8: 18.7)	(9.0; 14.7)

*Plasma samples were extracted with 2 ml methanol.

Samples taken at 0.67, 4, 10, 30, 60 and 120 min postinjection were analyzed for radioactive metabolite(s) and for unchanged radioligand, by adding the plasma (50–200 μl) to 2 ml methanol, sonicating, centrifuging and analyzing the supernatant by HPLC. Authentic (−)-5′-F-Δ^8-THC was added to the supernatant solution before HPLC. The retention time of (−)-F-Δ^8-THC in this system was 15 min.

RESULTS

Table 1 shows the time course distribution of (−)-5′^{18}F-Δ^8-THC in mice, expressed as % of injected radioactivity per organ as well as per gram of tissue. The uptake of the compound was highest at 5 min, with the liver, kidneys, small intestines and brain having the highest amounts of drug (20.07 ± 2.06, 7.33 ± 0.85, 3.42 ± 1.04 and 2.23 ± 0.34% of injected dose/g organ respectively). Radioactivity declined rapidly to approximately 25% of its peak value after 60 min in all tissues with the exception of the liver where it decreased to 37%. The small intestine was the only tissue where radioactivity increased seven hundredfold, indicating high concentration of THC in the feces.

All PET studies were performed in adult female baboons. Figure 1 shows the distribution of (−)-5′-^{18}F-Δ^8-THC in the primate brain 60 min after IV injection of the drug. These series of images represent horizontal slices of the baboon's skull and brain and they are separated from each other by 6.5 mm. The top of the figure represents the top of the skull and the bottom represents its basis. Areas that are colored deep red are areas high in radioactivity, while areas colored in purple have little radioactivity.

Uptake of the cannabinoid was analyzed from a series of images such as those described above, being taken from time 0 of the injection up to two hours from injection time. The images also allowed evaluation of the rate of accumulation as well as that of the clearance of the radioactivity in the various areas of the brain. The results are shown in Fig. 2. Uptake of the drug was similar in the basal ganglia, thalamus and cerebellum. The basal ganglia can be seen as the yellow area at the second row of images (Fig. 1), while the cerebellum is the lower yellow colored area in the third row of images (Fig. 1). Figure 2 shows that the drug accumulates rapidly (1.5% of injected dose/cc in 6 min) and is rapidly cleared (0.05% of injected dose/cc in 90 min) from these brain areas. The radioactivity at the base of the skull, seen as the deep red colored area in the third row of images in Fig. 1, identifies perhaps the sella turcica, which is a bony structure near which lies the pituitary. In this area radioactivity increased rapidly and then remained constant with time (2.3% of injected dose/cc in 12 min 2.5% of injected dose/cc in 90 min). This was explained as an indication of in vivo defluorination.

The fate of the drug in the animal was also studied through plasma analysis of the injected radioactivity. Table 2 shows the results obtained. It can be seen that with increasing time, the amount of dissociated ^{18}F radioactivity decreases (second column) but not as drastically as the amount of ^{18}F associated with the cannabinoid and its metabolites (third column) or (−)-5′-^{18}F-Δ^8-THC itself (fourth column). These results demonstrate relatively rapid metabolism of the drug associated mainly with defluorination. After 10 min, roughly only one-third of cannabinoid and its metabolites are still intact.

DISCUSSION

To our knowledge, (−)-5′-^{18}F-Δ^8-THC is the first cannabinoid positron-emitting derivative synthesized to date. This molecule was designed for visualizing cannabinoid binding sites in the primate brain using positron emission tomography imaging and was also used to study cannabinoid biodistribution in mice.

The results from the PET experiments discussed here show a number of similarities with those obtained by autoradiographical visualization of cannabinoid receptors in the brain using [^{3}H] CP-55,940. Both methods demonstrated the presence of cannabinoid binding sites in the basal ganglia and cerebellum. However, we also find some differences between the data from the two types of imaging methods. For example, our PET data do not reveal high localization of binding sites observed in the autoradiographic experiments. Conversely, the PET results show high concentration in the area of the thalamus while autoradiography reveals only modest binding there.

The results obtained from the PET experiments on the distribution of cannabinoid receptors in the brain do not distinguish between specific and nonspecific cannabinoid binding sites and in all likelihood represent the combined sum of the two. This could be due to the relatively low affinity of this natural cannabinoid when compared to that of [^{3}H] CP-55,940, which was the ligand used in the autoradiographic studies. PET experiments being currently planned will make use of ligands having higher affinities for the cannabinoid binding sites and should serve to refine the data described in this publication.

ACKNOWLEDGEMENTS

This work was supported by grants DA-3801 (A.M.) and DA-152 (A.M.) from the National Institute on Drug Abuse. PET experiments were performed at BNL under contract with the U.S. Department of Energy and supported by its office of Health and Environmental Research. The authors wish to acknowledge Dr. J. S. Fowler, E. Jellet, K. Karlstrom and C. Shea for advice and assistance. A.C. is a recipient of a Boehringer-Ingelheim award.

REFERENCES

1. Agurell, S.; Halldin, M.; Lindgren, J. E.; Ohlson, A.; Widman, M.; Gillspie, H.; Hollister, L. Pharmacol. Rev. 38:21–43; 1986.
2. Burstein, S.; Hunter, S.; Ozman, K. Prostaglandins and cannabis. Mol. Pharmacol. 23:121–126; 1983.

3. Charalambous, A.; Lin, S.; Marciniak, G.; Banijamali, A.; Friend, F. L.; Compton, D.; Martin, B. R.; Makriyannis, A. Pharmacological evaluation of halogenated Δ^{8}-THC analogs. Pharmacol. Biochem. Behav. 40:509–512; 1991.
4. Devane, W. A.; Dysarz, F. A., III; Johnson, R. M.; Melvin, L. S.; Howlett, A. C. Determination and characterization of a cannabinoid receptor in rat brain. Mol. Pharmacol. 34:605–613; 1988.
5. Dewey, W. L. Cannabinoid pharmacology. Pharmacol. Rev. 38: 151–178; 1986.
6. Dewey, S. L.; MacGregor, R. R.; Brodie, J. D.; Bendrien, B.; King, P. T.; Volkow, N. D.; Schlyer, D. J.; Fowler, J. S.; Wolf, A. P.; Gatley, S. J.; Hitzemann, R. Mapping muscarinic receptors in human and baboon brain using [N-11C-methyl]-benzotropin. Synapse 5:213–223; 1990.
7. Fowler, J. S.; Wolf, A. P. New directions in positron emission tomography. Annu. Rep. Med. Chem. 24:277–286; 1987.
8. Herkenham, M.; Lynn, A. B.; Little, M. D.; Johnson, R. M.; Melvin, L. S.; DeCosta, B. R.; Rice, K. C. Cannabinoid receptor localization in brain. Proc. Natl. Acad. Sci. USA 87:1932–1936; 1990.
9. Hershkovitz, M.; Goldman, R.; Raz, A. Effects of cannabinoids on neurotransmitter uptake, ATPase activity and morphology of mouse brain synaptosomes. Biochem. Pharmacol. 26:1327–1331; 1977.
10. Howlett, A. C. Cannabinoid inhibition of adenylate cyclase. Mol. Pharmacol. 27:429–436; 1985.
11. Makriyannis, A.; Banijamali, A.; Jarrell, H. C.; Yang, D. P. The orientation of (−)-Δ^{9}-tetrahydrocannabinol in DPPC bilayers as determined from solid state ^{2}H/NMR. Biochim. Biophys. Acta 986: 141–145; 1989.
12. Marciniak, G.; Charalambous, A.; Shiue, C.-Y.; Dewey, S. L.; Schlyer, D. J.; Makriyannis, A.; Wolf, A. P. ^{18}F-Labeled tetrahydrocannabinol: synthesis; and PET studies in a baboon. J. Lab. Comp. Radiophys. XXX:413–415; 1991.
13. Martin, B. R. Cellular effects of cannabinoids. Pharmacol. Rev. 38:45–74; 1986.
14. Matsuda, L.; Lolait, S. J.; Brownstein, M. J.; Yang, A. C.; Bonner, T. I. Structure of a cannabinoid receptor and functional expression of the cloned c.DNA. Nature 346:561–564; 1990.
15. Mavromoustakos, T.; Yang, D. P.; Charalambous, A.; Herbette, L. G.; Makriyannis, A. Study of the topography of cannabinoids in model membranes using x-ray diffraction. Biochim. Biophys Acta 1024:336–334; 1990.
16. Mechoulam, R. Cannabinoids as therapeutic agents. Boca Raton: CRC Press Inc.; 1986.
17. Nathan, T.; Yarom, A.; Drilansky, A.; Lander, N.; Livne, A. Cannabinoids and serotonin uptake by blood platelets: evidence for multiple sites of action. Biochem. Pharmacol. 31:439–441; 1982.
18. Pitt, C. G.; Hobbs, D. T.; Schvan H.; Twine, C. E., Jr.; Williams, D. L. The synthesis of deuterium, carbon-14 and carrier-free tritium labeled cannabinoids. J. Label. Comp. XI:551–575; 1975.